NANO LETTERS

pubs.acs.org/NanoLett

High-Efficiency Mechanical Energy Storage and Retrieval Using Interfaces in Nanowires

Suzhi Li,[†] Xiangdong Ding,[*,†] Ju Li,[*,†,‡] Xiaobing Ren,[†,§] Jun Sun,[†] and Evan Ma[*,†,∥]

[†]State Key Laboratory for Mechanical Behavior of Materials, Xi'an Jiaotong University, Xi'an 710049, China, [‡]Department of Materials Science and Engineering, University of Pennsylvania, Philadelphia, Pennsylvania 19104, [§]Ferroic Physics Group, National Institute for Materials Science, Tsukuba, 305-0047 Ibaraki, Japan, and [∥]Department of Materials Science and Engineering, Johns Hopkins University, Baltimore, Maryland 21218

ABSTRACT By molecular dynamics simulations, we demonstrate a new concept for mechanical energy storage and retrieval using surface energy as reservoir in body-centered cubic (bcc) tungsten nanowire, achieving a combination of unique features such as large and constant actuation stress (>3 GPa), exceptionally large actuation strain (>30%) and energy density, and >98% energy storage efficiency. The underlying mechanism is a shear-dominant diffusionless transformation akin to martensitic transformation, but driven by surface rather than bulk free energies, and enabled by motion of coherent twin boundary, whose migration has been shown to possess ultralow friction in bcc metals. Aside from energy storage, such surface-energy driven displacive transformations are important for phase transformation and energy-matter control at the nanoscale.

KEYWORDS Surface energy, displacive transformation, dissipation, twin boundary migration, pseudoelasticity

Advances in information and nano/bio technologies demand novel materials and approaches for energy storage and conversion with high efficiency. One recent attempt to harness the fluctuating and transient mechanical energy around us (such as that in the vibrations and in living bodies) is the development of "nanogenerators" to convert mechanical energy into electrical energy using piezoelectric ZnO nanowire arrays.[1,2] In the following, we demonstrate a nanowire array that stores mechanical energy by using the free surfaces as a reservoir, and vice versa, retrieves mechanical work from the surface energy, with unique actuation characteristics and exceedingly high efficiency.

The mechanism we exploit is an ultralow friction surface-energy driven displacive transformation (SEDDT) of nanoscale crystals. Solid-to-solid transformations are generally either diffusive or displacive, or combination of the two.[3,4] Diffusive transformations are mediated by registry-randomizing redistribution (diffusion) of atoms, whereas displacive transformations rely on more ordered cooperative movements of many atoms, such as dislocation glide[5] or interfacial migration,[6−8] to induce changes in the crystal shape and/or structure. Examples of displacive transformations include martensitic transformation in shape memory alloys (SMAs)[9] and deformation twinning.[10] In conventional materials, nearly all the structural transformations we are familiar with, diffusive or displacive, have high dissipative loss, except for elastic deformation that only sustains a low-stored energy density. Even for the pseudoelastic TiNi SMAs with excellent shape recovery ability, around 50% of the input energy will be lost.[11] Recent investigations have shown that certain dislocation glide processes in nanocrystals[12] and nanotubes[13] and twin boundary migration[6−8] in face-centered cubic (fcc) nanowires[14,15] can provide strain recovery similar to the shape memory effect/pseudoelasticity in SMAs, but the energy loss is also high, exceeding 80 and 40%, respectively.

Our approach exploits displacive transformations driven by surface energy in small-volume materials,[14,15] a paradigm different from displacive transformations in bulk materials, which are usually driven by bulk free energy (as in temperature-induced martensitic transformation[3]) or bulk elastic energy (as in pseudoelasticity of SMAs[9] and dislocation plasticity[5]). To achieve low dissipation, that is, to minimize the difference between the input and the output energies, here we choose body-centered cubic (bcc) tungsten (W) nanowires as the candidate material. There are several reasons for selecting this material. First, previous ab initio calculations of the multiplane generalized stacking fault (MGSF)[16] energy for deformation twinning have revealed unique features in bcc metals,[17] indicating a dramatic difference from fcc metals. The energy landscape for fcc twinning is always very rugged no matter how thick the twin is. In contrast, in bcc metals, once a twin embryo exists with thickness >5 layers, the twin boundary's shear-coupled migration has ultralow friction with very low migration barrier energy (only 40 mJ/m^2 in the case of molybdenum[17]). This means a twinning partial dislocation gliding on top of a twin embryo >5 layers thick would have very low dislocation core energy, very wide core, and ultralow lattice friction.[17] The flat energy landscape for W twin boundary migration will be demonstrated later in this paper. Second, to suppress

*To whom correspondence should be addressed. E-mail: (X.D.) dingxd@mail.xjtu.edu.cn; (J.L.) liju@seas.upenn.edu; (E.M.) ema@jhu.edu.

Received for review: 01/24/2010
Published on Web: 04/06/2010

DOI: 10.1021/nl100263p | *Nano Lett.* **2010,** *10,* 1774–1779

diffusive processes that compete with SEDDT and may destroy the nanostructures, diffusion should be minimized. We therefore choose a refractory material with very high melting temperature (3695 K), such that during the room-temperature cycling of the device the amount of diffusion would be negligible. Third, since we are exploiting controlled twin boundary migration[6−8] rather than ordinary dislocation glide based plasticity,[5] ordinary dislocation processes must also be suppressed. bcc metals are advantageous in this regard as well due to the large lattice friction (Peierls stress) against screw dislocation glide.[18−20] As such, a wide temperature-sizescale window is available in bcc metals where twin-boundary migration based SEDDT is the softest mode and dominates over other dissipative processes.

Next we demonstrate the feasibility of our approach by using molecular dynamics (MD) simulations of a single-crystal bcc W nanowire. The Finnis-Sinclair (FS) potential,[21] which reproduces the properties (such as cohesive energy, elastic constants, low-index surface energies) of bcc W quite well, was utilized in the MD simulations. The W nanowire, in the x-[100], y-[011], z-[0$\bar{1}$1] orientations, had initial dimensions $50a_0 \times 5\cdot 2^{1/2}a_0 \times 5\cdot 2^{1/2}a_0$ (15.83 nm × 2.24 nm × 2.24 nm), where $a_0 = 3.165$ Å is the lattice constant of W at 0 K. The nanowire was relaxed at room temperature for 100 ps. It was then loaded in the x ([100]) direction with atoms in the three ending layers fixed to play the role of loading grips, while other atoms move freely and interact with their neighbors. The tensile straining was performed at a prescribed strain increment of 0.1 % by applying the small magnitude of displacement to the loading grips, followed by relaxation at the present strain for 80 ps, and the stress was evaluated by averaging over the last 20 ps. Unloading was performed in a similar way by applying a negative strain. The MD simulation was carried out using the LAMMPS code.[22]

Figure 1a shows the stress−strain curve of the [100] W nanowire with a side width of 2.3 nm (hereafter referred to as 2.3 nm W nanowire) upon a loading and unloading cycle at 300 K. The wire deforms elastically until a stress level of 16 GPa, after which the stress drops dramatically, followed by a long plateau with an almost constant stress of ∼3.5 GPa and a large inelastic strain of >30 %. Upon unloading, the nanowire can fully recover to the original position before loading, exhibiting a classic pseudoelastic behavior with the total recoverable strain exceeding 40 %.

At the atomic level, twinning/detwinning is the underlying mechanism responsible for the reversible strain. As shown in Figure 1(b), during the tensile loading a single twin nucleates in the center, dividing the wire into three domains. Atoms in the original and the newly formed domains mirror each other with respect to the twin boundaries, as shown in Figure 1c. Loading drives the twin growth gradually toward the ends, and finally the whole wire except for the fixed ends transforms to a new lattice orientation of x-[011], y-[100], z-[0$\bar{1}$1] (90° rotation of the unit cell in xy plane). For

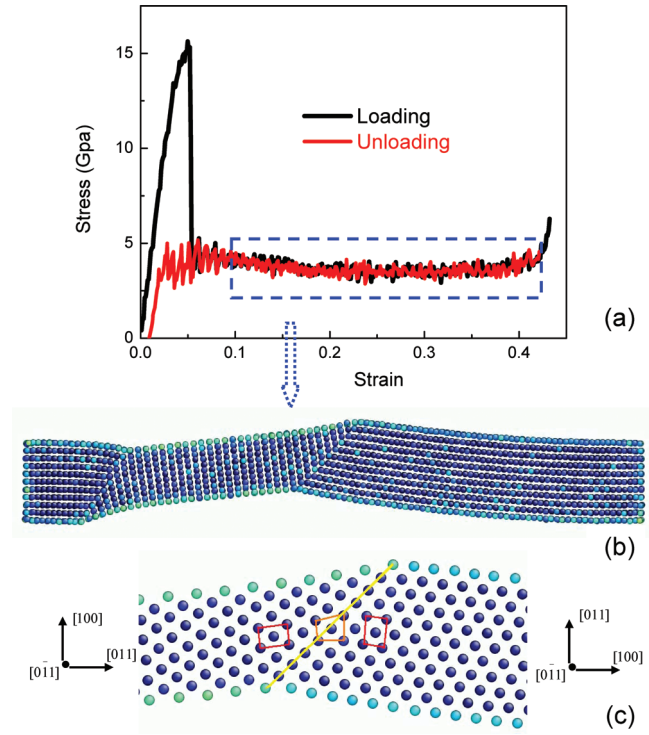

FIGURE 1. Pseudoelastic behavior of a 2.3 nm (side width) bcc tungsten [100] nanowire. (a) Stress−strain curves upon loading and unloading at 300 K. (b) Deformation twinning during loading/unloading, where a segment of wire in the middle is transformed to [011] configuration. (c) Atomic configuration near a twin boundary. Shear-coupled migration[6−8] of this twin boundary will produce lattice reorientation, shown by the two unit cells in red rectangles.

convenience, hereafter we refer to the initial and reoriented configurations as the [100] and [011] wire, respectively. When the system is unloaded, detwinning follows the reverse route to recover the wire to its original shape with complete recovery of the original atomic registries, indicating it is a diffusionless transformation.

The nanowire has a large surface-to-volume ratio and surface free energy plays a key role. Compared with the [100] wire configuration, the reoriented [011] wire configuration has a higher surface energy per atom, providing the driving force to transform back to the [100] configuration upon unloading. Figure 2a shows the excess energy per atom (with respect to bulk reference) of the perfect [100] and the reoriented [011] wires as a function of the wire size at 300 K. The energy difference increases with decreasing wire size as $\propto 1/d$, where d is the original wire width, indicating that the excess energies are caused physically by surface energies. Note that the energy difference shown in Figure 2a is the reservoir that mechanical work is converted to (released from) during loading (unloading), in the plateau regions of Figure 1a.

We now analyze the energy dissipation mechanisms in the W nanowire. There is a large hysteresis in the strain range of 0−9 % in Figure 1a, which corresponds to the

DOI: 10.1021/nl100263p | *Nano Lett.* **2010,** *10,* 1774–1779

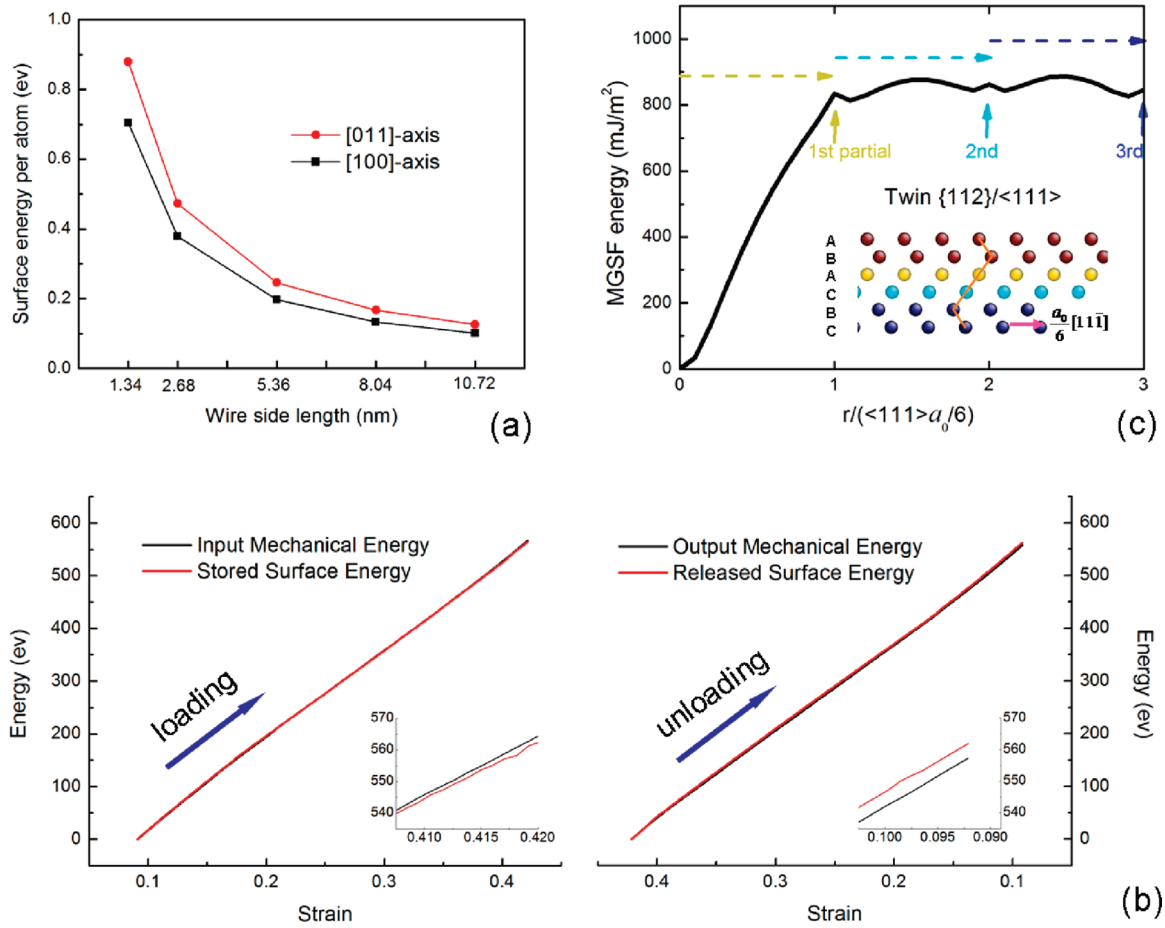

FIGURE 2. (a) The size-dependent excess energy per atom (in reference to bulk) between [100] and [011] W nanowire configurations at 300 K. (b) Energy change during loading and unloading of a 2.3 nm W nanowire. During the loading process, almost all the input mechanical work is converted to the increased surface energy. Upon unloading, the stored surface energy will be transformed back to mechanical work with little loss. (c) Multiplane generalized stacking fault (MGSF) energy curve in W crystal. When viewed along ⟨110⟩, bcc crystal has an ABCABC stacking sequence. $\langle 111\rangle a_0/6$ partial dislocations emitted on consecutive {112} planes will lead to stacking-sequence change (ABACBC), and the nucleation and growth of a nanotwin.

creation and annihilation of the twin boundaries. A key observation is that over a wide plastic strain range (9−42 %), the hysteresis is exceptionally small. In the highlighted range (blue box), the loss is only 2 %, as shown in Figure 2b, which compares the input/output work with the stored surface energy. By taking the initial state (strain 0.09) of the blue box as a reference, the input/output work was calculated by integrating over stress in the plateau stage upon loading/unloading, which is 567.0 and 557.3 eV, respectively (shown in Figure 2b). The total surface energies can be calculated independently by looking at stress-free nanowires. As will be shown, upon loading, almost all the input work was transformed into excess surface energy, whereas upon unloading, almost all the stored surface energy was converted back to useful mechanical work. The small difference between the released surface energy and the output mechanical work is attributed to elastic energy in the material and energy dissipation for twin boundary motion.

This extraordinary energy efficiency is due to the unique multiplane generalized stacking fault (MGSF) energy pathway of bcc metals, including W. The twin growth/shrinkage is mediated by a series of $\langle 111\rangle a_0/6$ partial dislocations in the adjacent {112} planes, Figure 2c. Here the initial three partials are considered, to illustrate the point. The W MGSF energy curve, which is consistent with that obtained from ab initio calculation for bcc Mo,[17] shows a flat landscape after the first major energy barrier. This indicates that after the first pair of partial dislocations separate during twin nucleation, the creation and motion of subsequent twinning partials are very easy. As such, the work done is mostly associated with the nondissipative changes in the surface energy, and only a very small part is used to drive the migration of the twin boundary. On the basis of the above, we can further obtain the stress needed for moving the pre-existing twin boundary as follows

$$\sigma_{\text{load}}^{\text{SEDDT}} \approx \frac{K}{d} + \sigma_{\text{loss}},\ \sigma_{\text{unload}}^{\text{SEDDT}} \approx \frac{K}{d} - \sigma_{\text{loss}},\ \sigma_{\text{loss}} > 0 \quad (1)$$

DOI: 10.1021/nl100263p | *Nano Lett.* **2010,** *10,* 1774–1779

TABLE 1. Comparison of Various Smart Materials[9,15,26,27] with our 2.3 nm W Nanowire

typical actuator (examples)	strain (%)	stress (MPa)	energy efficiency (%)	energy density (J/cm^3)
piezoelectric ceramics (PZT)	0.2	110	90	0.1
electroactive polymer (silicone)	63	3	90	0.75
shape memory alloy (TiNi)	5−10	800	<50	>100
megnetostrictive (Terfenol-D)	1	700	80	0.025
fcc shape memory nanowire (Cu)	50	5500	41	930
bcc nanowire (W)	>30	3500	98	>1000

where K is a coefficient [$= (2 \cdot 2^{1/2}\gamma_{100} - 2\gamma_{110})/(2^{1/2} - 1)$, where γ_{100} and γ_{110} are the surface energies of the $\{100\}$ and $\{110\}$ planes, respectively], which is related to the surface energy difference between the [100] and [011] wires, and K/d is the constant background stress due to the surface configuration change.[23,24] The second term (σ_{loss}) is the dissipative frictional stress to drive twin boundary migration.

For the present calculation in Figure 1, $\gamma_{100} = 2.92$ J/m^2, $\gamma_{110} = 2.57$ J/m^2, and $d = 2.3$ nm, then the value of K/d at 300 K is 3.3 GPa, which is very close to the plateau stress (3.5 GPa) in Figure 1. The error mainly comes from the elastic stretching and bending energy of the nanowires which was neglected in eq 1.

Therefore, the loss ratio during a loading/unloading cycle can be approximately calculated as

$$\eta \approx \frac{\sigma_{\text{load}}^{\text{SEDDT}} - \sigma_{\text{unload}}^{\text{SEDDT}}}{K/d} \tag{2}$$

From the above, it is clear that in order to reduce dissipation in SEDDT, σ_{loss} needs to be small compared to K/d, where K is size-independent. In the Figure 1 simulation, $\sigma_{\text{loss}} \approx 30$ MPa. Mechanistically σ_{loss} is due to either finite mobility of twin partial dislocation inside the nanowire, or nucleation of twin partial dislocation from the nanowire surface. σ_{loss} is very small here because twinning partials in bcc metals have very wide cores, low core energies, and low Peierls stresses, due to the flat MGSF landscape predicted by ab initio calculations.[17] If twin-partial-dislocation mobility controls σ_{loss}, it would be d-independent; if twin-partial-dislocation nucleation controlled, σ_{loss} may only be weakly d-dependent due to the number of possible thermally activated dislocation nucleation sites on the nanowire surface.[25] On the other hand, σ_{loss} is certainly temperature and strain-rate dependent:[6,25] $\sigma_{\text{loss}} = \sigma_{\text{loss}}(T, \dot{\varepsilon})$. In our simulations both the loading and unloading were performed at an exceptionally high strain rate $\dot{\varepsilon} \sim 10^7$/s. $\dot{\varepsilon}$ in experimental conditions would be much lower, therefore we expect σ_{loss}, and consequently η, to be much lower than 2% in experiments. The MD simulations here only provide an upper bound to η, which is very low already. As for the wire size effects, eq 2 suggests that as long as the nanowires have d less than ~5 nm, the energy efficiency ($1 - \eta$) would remain over 95% and superior to other smart materials; see Table 1.

Understanding the above principles, we now proceed to propose a design for permanent storage of mechanical energy. This mechanical energy storage device (MESD) is somewhat similar to actuators. Recent developments in information technology, nanotechnology, and biotechnology present an increasing need for miniaturization and long lifetime devices that can produce (a) large actuation stress, (b) high actuation strain, (c) high-energy density, and (d) high-energy efficiency (low loss). We have summarized the performances of other candidate "smart materials", such as piezoelectric ceramics, electroactive polymers, shape memory alloys and magnetostrictive materials, in Table 1.[9,15,26,27] We see that piezoelectric materials[1,2] provide high efficiency and long lifetime, but small actuation strains. Electroactive polymers show high actuation strains and efficiency, but low actuation stress and energy density. For traditional SMAs, energy loss is a big problem, although their other properties are pretty good.

Our task is to build an MESD based on SEDDT and twin boundary migration. Since the main source of hysteresis in Figure 1 is the creation and annihilation of two twin boundaries, our new design uses a single preexisting twin boundary that cannot annihilate. The design is shown in Figure 3a, which may be carved or etched out of a bcc bicrystal[28] that has a preexisting twin boundary by electron lithography or focused ion beam (FIB).[29]

We first show the behavior of a $d = 2.3$ nm nanowire with a preexisting single twin boundary. As shown in Figure 3a, atoms in red color were fixed to play the role of the loading grip, the yellow ones were taken as the transition area to avoid stress concentration near the ends, and the middle blue part is the functional portion of the device. It works like an accordion; when we applied a uniaxial tensile loading to the wire, the twin boundary moves toward the right end, while upon unloading, the motion reverts back in the opposite direction. The corresponding stress−strain curve during the loading/unloading cycle is displayed in Figure 3b, showing small hysteresis and a <2% energy loss, which is similar to the performance of the previous defect-free nanowire in the strain range of 9−42% (Figure 1a). Compared with the other materials in Table 1, the present MESD provides all-around desirable features, including a high and constant actuation stress approaching 3.5 GPa, large recoverable strain exceeding 30%, high energy density, high efficiency (98%), as well as miniaturization at the nanoscale. To illustrate that our design can be scaled up, we constructed

DOI: 10.1021/nl100263p | *Nano Lett.* **2010,** *10,* 1774--1779

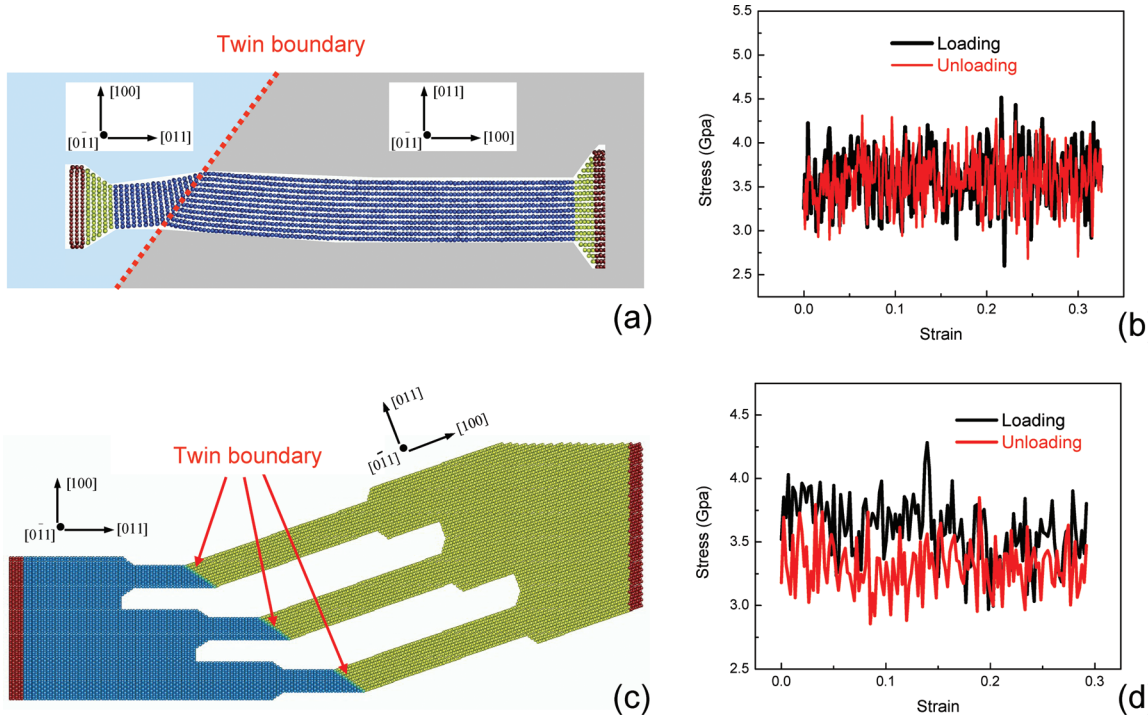

FIGURE 3. (a) W nanowire (2.3 nm) with a pre-existing twin boundary (TB). This setup can be fabricated from a bcc bulk bicrystal by electron lithography or FIB.[29] The red dot line is the boundary, dividing the wire into two crystals with mirrored orientations. Atoms in red color were fixed to play the role as loading grip, the yellow ones were taken as the transition area to avoid stress concentration near the ends, and the middle blue part is the nanowire with a pre-existing TB. (b) Stress−strain curve upon loading and unloading cycle of this single nanowire. A movie of the operation of this single nanowire device is shown in Movie M1 (Supporting Information). (c) bcc W nanowire array. (d) Stress−strain curve upon loading and unloading at 300 K in W nanowire array. A movie of the accordion-like operation of this nanowire array is shown in Movie M2 (Supporting Information).

in Figure 3c a nanowire array, and perform MD simulations of its loading/unloading. From the corresponding stress−stain curve at 300 K shown in Figure 3d, this array performs much like the single wire in Figure 3a. Cyclic, accordion-like operations of the single-nanowire and nanowire-array MESD are shown in Movie M1 and M2, respectively, in Supporting Information.

Because SEDDT relies on surface energies, it would be sensitive to surface oxidation. Oxidation will change the effective surface energies γ_{100} and γ_{110}, thus changing K in eq 1. It will also introduce extra source of dissipation when the device is mechanically cycled. Fortunately, vacuum packaging technology in MEMS is becoming more mature,[30−32] which can be accomplished at both the package level and the chip/wafer level. Well-known devices such as the vacuum tube and incandescent light bulb do use W and require vacuum.

In summary, using MD simulations we have demonstrated the unique features of a surface-energy driven displacive transformation (SEDDT) in simple bcc metallic nanowires. Once a twin boundary is present in the bcc nanowire, shear-coupled twin boundary migration[6−8] is a reversible, ultralow-friction process that mediates the two-way conversion between mechanical work and excess surface energy. The design provides highly efficient energy storage, with large recoverable strain, high constant stress and other functional properties superior to existing materials for nanoelectro-mechanical systems. In addition to energy storage and actuation, understanding SEDDT in metallic and nonmetallic materials may provide new avenues for controlling phase transformation and functional properties of nanoscale materials, for example, nonvolatile and ultralow power information storage by phase change[33] and/or surface configuration change.

Acknowledgment. This work was supported by the grants from NSFC (50771079, 50720145101, and 50831004) and 973 Program of China (2010CB631003). We also appreciate the support from the 111 Project as well as NCET of China. J.L. appreciates the support by NSF CMMI-0728069 and DMR-0520020, AFOSR FA9550-08-1-0325 and ONR N00014-05-1-0504. The work of E.M. was carried out under an adjunct professorship at XJTU and supported in part by US-NSF-DMR-0904188.

Supporting Information Available. The loading/unloading process in the single W nanowires and nanowire arrays in movies of M1 and M2, respectively. This material is available free of charge via the Internet at http://pubs.acs.org.

REFERENCES AND NOTES

(1) Wang, Z. L.; Song, J. H. *Science* **2006**, *312* (5771), 242–246.
(2) Yang, R. S.; Qin, Y.; Dai, L. M.; Wang, Z. L. *Nat. Nanotechnol.* **2009**, *4* (1), 34–39.

DOI: 10.1021/nl100263p | *Nano Lett.* **2010,** *10,* 1774–1779

(3) Christian, J. W. *The Theory of Transformations in Metals and Alloys*, 3rd ed.; Elsevier: Amsterdam, 2002.
(4) Suresh, S.; Li, J. *Nature* **2008**, *456* (7223), 716–717.
(5) Hirth, J. P.; Lothe, J. *Theory of dislocations*, 2nd ed.; Wiley: New York, 1982.
(6) Cahn, J. W.; Mishin, Y.; Suzuki, A. *Acta Mater.* **2006**, *54* (19), 4953–4975.
(7) Zhang, H.; Duy, D.; Srolovitz, D. J. *Philos. Mag.* **2008**, *88* (2), 243–256.
(8) Rupert, T. J.; Gianola, D. S.; Gan, Y.; Hemker, K. J. *Science* **2009**, *326* (5960), 1686–1690.
(9) Otsuka, K.; Ren, X. *Prog. Mater. Sci.* **2005**, *50* (5), 511–678.
(10) Chen, M. W.; Ma, E.; Hemker, K. J.; Sheng, H. W.; Wang, Y. M.; Cheng, X. M. *Science* **2003**, *300* (5623), 1275–1277.
(11) San Juan, J.; No, M. L.; Schuh, C. A. *Nat. Nanotechnol.* **2009**, *4* (7), 415–419.
(12) Rajagopalan, J.; Han, J. H.; Saif, M. T. A. *Science* **2007**, *315* (5820), 1831–1834.
(13) Mori, H.; Ogata, S.; Li, J.; Akita, S.; Nakayama, Y. *Phys. Rev. B* **2007**, *76* (16), 165405.
(14) Park, H. S.; Gall, K.; Zimmerman, J. A. *Phys. Rev. Lett.* **2005**, *95* (25), 255504.
(15) Liang, W. W.; Zhou, M. *Phys. Rev. B* **2006**, *73* (11), 115409.
(16) Ogata, S.; Li, J.; Yip, S. *Science* **2002**, *298* (5594), 807–811.
(17) Ogata, S.; Li, J.; Yip, S. *Phys. Rev. B* **2005**, *71* (22), 224102.
(18) Ismail-Beigi, S.; Arias, T. A. *Phys. Rev. Lett.* **2000**, *84* (7), 1499–1502.
(19) Woodward, C.; Rao, S. I. *Phys. Rev. Lett.* **2002**, *88* (21), 216402.
(20) Li, J.; Wang, C. Z.; Chang, J. P.; Cai, W.; Bulatov, V. V.; Ho, K. M.; Yip, S. *Phys. Rev. B* **2004**, *70* (10), 104113.
(21) Finnis, M. W.; Sinclair, J. E. *Philos. Mag. A* **1984**, *50* (1), 45–55.
(22) Plimpton, S. *J. Comput. Phys.* **1995**, *117* (1), 1–19.
(23) Diao, J. K.; Gall, K.; Dunn, M. L.; Zimmerman, J. A. *Acta Mater.* **2006**, *54* (3), 643–653.
(24) Diao, J. K.; Gall, K.; Dunn, M. L. *Nat. Mater.* **2003**, *2* (10), 656–660.
(25) Zhu, T.; Li, J.; Samanta, A.; Leach, A.; Gall, K. *Phys. Rev. Lett.* **2008**, *100* (2), No. 025502.
(26) Wei, Z. G.; Sandstrom, R.; Miyazaki, S. *J. Mater. Sci.* **1998**, *33* (15), 3743–3762.
(27) Kornbluh, R.; Pelrine, R.; Pei, Q. B.; Oh, S.; Joseph, J. *Smart Structures and Materials 2000: Electroactive Polymer Actuators and Devices (Eapad)* **2000**, *3987*, 51–64.
(28) Gemperlova, J.; Jacques, A.; Gemperle, A.; Vystavel, T.; Zarubova, N.; Janecek, M. *Mater. Sci. Eng., A* **2002**, *324* (1−2), 183–189.
(29) Reyntjens, S.; Puers, R. *J. Micromech. Microeng.* **2001**, *11* (4), 287–300.
(30) Esashi, M. *J. Micromech. Microeng.* **2008**, *18* (7), No. 073001.
(31) Ramesham, R.; Kullberg, R. C. *J. Micro/Nanolithogr., MEMS, MOEMS* **2009**, *8* (3), No. 031307.
(32) Gan, Z. Y.; Huang, D. X.; Wang, X. F.; Lin, D.; Liu, S. *Sens. Actuators A* **2009**, *149* (1), 159–164.
(33) Lee, S. H.; Jung, Y.; Agarwal, R. *Nat. Nanotechnol.* **2007**, *2* (10), 626–630.

DOI: 10.1021/nl100263p | *Nano Lett.* **2010,** *10,* 1774–1779